Physica C 169 (1990) 294–298
North-Holland

ELECTRON TUNNELING IN SUPERCONDUCTING $Ba_{0.6}K_{0.4}BiO_3$

F. MORALES and R. ESCUDERO
Instituto de Investigaciones en Materiales, Universidad Nacional Autónoma de México, Apartado Postal 70-360, México, D.F. 04510, Mexico

D.G. HINKS and Y. ZHENG
Materials Science Division, Argonne National Laboratory, Argonne, Illinois 60439, USA

Received 2 May 1990
Revised manuscript received 18 June 1990

We report tunneling measurements using superconducting bulk samples of $Ba_{0.6}K_{0.4}BiO_3$ and evaporated counterelectrodes of Sn. With our procedure, we find reproducible tunneling characteristics that show the gap feature and high frequency structure in the dI/dV versus V curves. This structure may be related to the phonon spectrum or to the excitations that give rise to superconductivity in these ceramic materials. The energy gap evolution with temperature follows BCS-like behavior, with ratio $2\Delta/K_BT_c$ at $T=0$ K in the range of intermediate coupling.

1. Introduction

The discovery of superconductivity in $Ba_{1-x}K_xBiO_3$ provides the possibility of comparing its characteristics to conventional phonon mediated superconductors and to the new Cu-based, high-T_c materials [1]. This compounds has received much attention because it is the first oxide superconductor without Cu in which the transition temperature, T_c, is of the order of 30 K, well above the best A-15 strong coupled superconductors. The crystal structure of this compound is a simple-cubic perovskite formed from corner-shared BiO_6 octahedra with Ba and K on the cell origin [2,3]. This three dimensional structure is isotropic with no magnetism and, therefore, the pairing mechanism might be totally different from the Cu–O based compounds where magnetic interactions or low dimensional behavior could be responsible for the superconducting state. Early oxygen isotropic effect measurements in the Ba–K–Bi–O system have led to large values of α_{ox} that imply a phonon-mediated pairing mechanism [4]. Calculation on the thermodynamic properties of this compound by Navarro and Escudero, using Eliashberg gap equations, confirm the strong coupling behavior of this compound similar to Nb_3Ge, a typical intermetallic superconductor [5]. Raman spectroscopy shows an optical phonon at 348 cm^{-1} (43 meV) with a Fano lineshape indicative of strong coupling between this phonon and the electron spectrum. For a non-superconducting sample of the material at a lower potassium content, the same phonon is not observed to be coupled to the electronic states [6]. Superconducting energy gap measurements, using infrared spectroscopy [7] and tunneling measurements [8], are consistent with a coupling constant, $2\Delta/K_BT_c$, in the range of 3.5 to 5.8. The tunneling results [8] show broad gap structure due to the apparent large lifetime broadening effects. More tunneling data is required to understand this apparent broadening of the superconducting gap in these materials.

Further the excitation spectrum that can be obtained from available tunneling measurements (from the differential conductivity and the derivative of the differential conductivity) must be explored. This spectroscopic technique, which is the most informative probe of the superconducting state, senses the microscopic processes which form the superconducting condensate, and can give information to completely characterize the superconducting state.

The information that can be extracted from tunneling experiments is: the temperature dependence of the energy gap, the phonon density of states, the coupling function $\alpha^2(\omega)F(\omega)$, etc. However, reliable tunneling data in these new ceramic materials have been very difficult to obtain. This is mainly due to the problem of making reproducible tunnel junctions. These particular difficulties are attributable to the nature of the parameters that are involved in these high-T_c superconductors, such as the small coherence length, ξ_0, the rapid surface degradation, and possible changes in oxygen stoichiometry.

In this paper we report on tunneling experiments with these materials which give information on the size of the energy gap and the structure of the excitation spectrum.

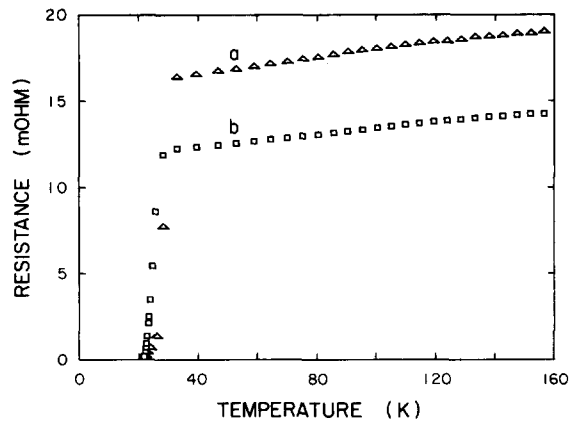

Fig. 1. Resistance vs. temperature for a sample of $Ba_{0.6}K_{0.4}BiO_3$: (a) as received, (b) after junction fabrication.

2. Experimental

The tunneling measurements were done using bulk ceramic material with the composition $Ba_{0.6}K_{0.4}BiO_3$. The melt processed sample was prepared as reported by Hinks et al. [3]. The tunnel junctions were conventional, sandwich type metal–insulator–superconductor (MIS) junctions. A pellet of high density material was encapsulated in high vacuum epoxy. Once the epoxy had cured, the surface of the pellet was polished and cleaned with an etching solution described by Gurvitch et al. [9]. After the cleaning procedure, the surface was left in the laboratory atmosphere for about 24 h. The junctions were completed by evaporating a thin strip of Sn as the counterelectrode. The junction dimensions were approximately 0.1×1.0 mm^2 with differential resistances (zero bias) of between 20 to 100 Ω. The tunnel junctions were measured at different temperatures between 4 and 300 K. In order to check that the material was still superconducting after fabrication of the junction, the resistance versus temperature characteristic was measured and compared to the material as received. As can be observed in fig. 1, the onset temperature (≈ 30 K) and the zero resistance (21 K) of the as-received material was not changed indicating no degradation occurred during fabrication.

The measurements on the tunnel junctions were done using the conventional modulation technique. The differential resistance (dV/dI) and the first derivative, d^2V/dI^2, versus voltage show interesting features which can be related to the energy gap, Δ. The measurements also display structure at higher voltages which is, in conventional superconductors, the signature of phonon interactions with quasiparticles. The conductance (the inverse of the differential resistance) is proportional to the density of states in the superconducting state. The second harmonic, d^2V/dI^2, gives information about the coupling function $\alpha^2(\omega)F(\omega)$. Dips in d^2V/dI^2 will correspond to peaks in the coupling function once the energy scale is corrected by $\omega - \Delta$.

The conductance versus voltage characteristics of a typical tunnel junction of $Ba_{0.6}K_{0.4}BiO_3$–I–Sn taken at different temperatures above T_c, are shown in fig. 2. The curve at 200 K can be considered as the normal state, in the sence that it shows typical parabolic behavior. Also a small, negative offset is observed, which can be explained assuming a different average barrier height at each side of the insulating barrier as proposed by Brinkman et al. [10]. At 77 K and below, the conductance shows an extra feature. The parabolic background remains but an increase in the conductance around zero volts becomes more and more noticeable as the temperature decreases. This anomalous *normal state* was also observed by Zasadzinski [11] in his tunneling experiments, in the material with $x=0.375$. There is no explanation for this feature, although recent theoretical work reports a similar behavior in systems with interacting charge

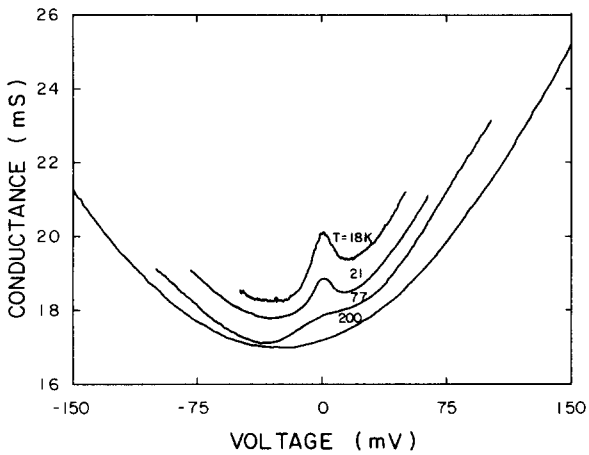

Fig. 2. Conductance vs. voltage curves (vertically shifted) for a $Ba_{0.6}K_{0.4}$ BiO_3–insulator–Sn junction in the normal state at different temperatures.

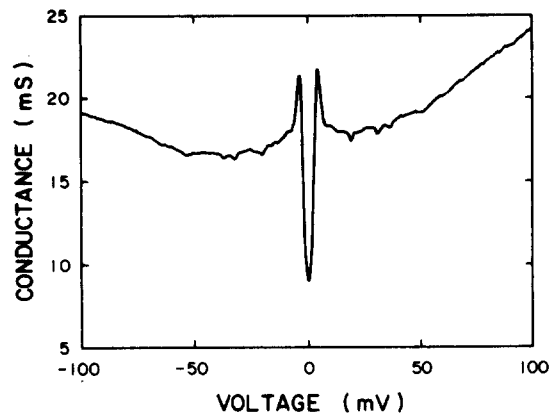

Fig. 3. Conductance vs. voltage of the $Ba_{0.6}K_{0.4}BiO_3$–insulator–Sn tunnel junction measured at 4 K.

density waves and superconductivity [12]. Note that the zero resistance transition temperature, as indicated in fig. 1, occurs at 21 K, but the conductance curves at 21 and 18 K do not show the opening of an energy gap. One logical explanation for this behavior is the well known fact that tunneling senses regions in the sample to a depth related to the coherence length in contrast to the resistance measurement which senses the bulk percolative length.

Figure 3 shows the conductance vs. voltage characteristic of the same tunnel junction at 4 K. The curves shows the energy gap and structure from 10 to 70 mV. Figure 4 shows a set of dI/dV versus V curves taken from 4 to 21 K with the curves displaced vertically for clarity. The data have two interesting features: first, the evolution of the minimum of the conductance curve, $G(0)$, with temperature and, second, the evolution of the high frequency symmetrical structure on both sides of the gap region. The dependence of $G(0)$ with temperature could be correlated with increasing the electronic density of states inside the energy gap as the temperature is increased. After normalizing the curves shown in figure 4 with the characteristic dI/dV at 18 K, we plotted the relative depression of the $G(0)$ as $1-G(0)$ versus T/T_c in fig. 5. Figure 6 shows the conductance of the tunnel junction at 4 K normalized with data at 18 K. The energy gap, Δ, can be determined using a smeared BCS density of states, given by $N_s(E)=\mathrm{Re}\{E-i\Gamma)/[(E-i\Gamma)^2-\Delta^2]^{1/2}\}$. In this equation Γ is a parameter which may be related to the density of states inside the gap, and was proposed by Dynes et al. to account for lifetime effects [13]. The values for Δ and Γ in this equation that fit the experimental result of fig. 6 are $\Delta=2.9$ meV, and the smeared parameter $\Gamma=1.6$ meV. Using the same fitting routine we can extract the energy gap development with temperature, which is shown in fig. 7. In fig. 7 we plotted the energy gap normalized to the value of 4 K. The error bars mark the uncertainty in the measurement. The temperature scale is also nor-

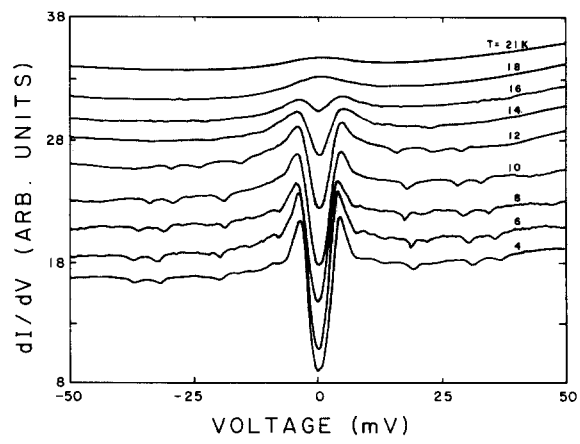

Fig. 4. Conductance vs. voltage curves taken from 4 to 21 K for the $Ba_{0.6}K_{0.4}BiO_3$–insulator–Sn junction. The curves have been displaced vertically for clarity.

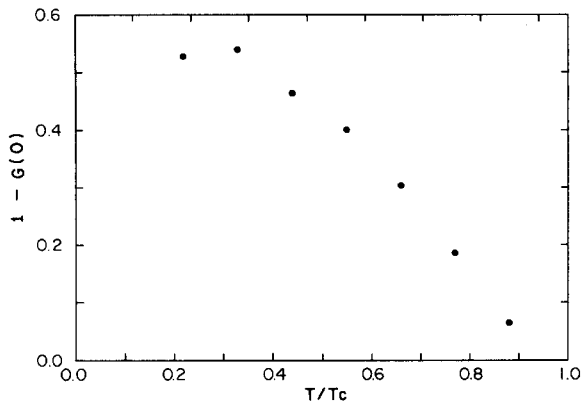

Fig. 5. The relative depression of the zero bias normalized conductance $G(0)$ plotted as $1-G(0)$ vs. T/T_c for the $Ba_{0.6}K_{0.4}BiO_3$–insulator–Sn junction. T_c was taken as 18 K.

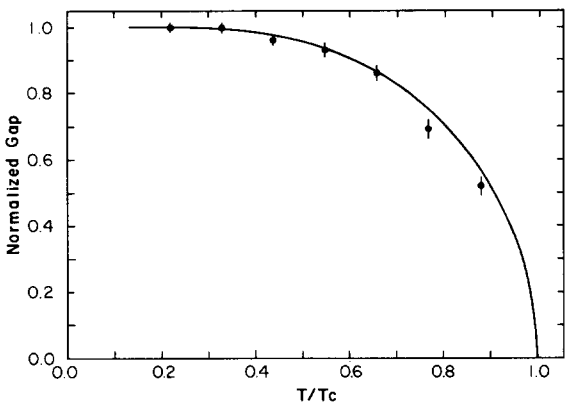

Fig. 7. Temperature variation of the normalized energy gap $\Delta(T)/\Delta(4\text{ K})$ for $Ba_{0.6}K_{0.4}BiO_3$ with $T_c=18$ K. The solid line represents the temperature dependence of the BCS theory.

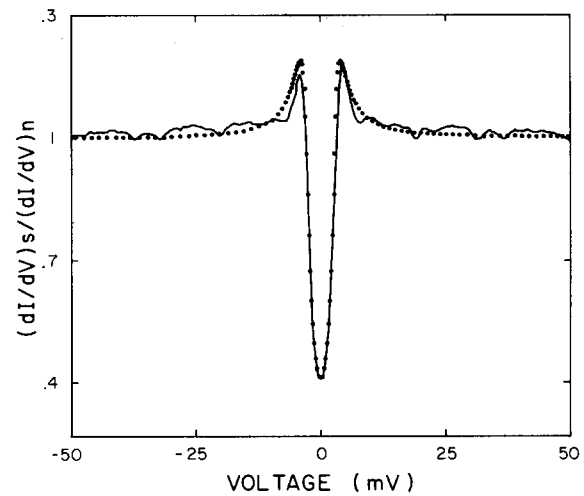

Fig. 6. Normalized conductance curve at 4 K normalized to 18 K for the $Ba_{0.6}K_{0.4}BiO_3$–insulator–Sn junction. The dotted curve is a smeared BCS density of states with $\Delta=2.9$ meV and $\Gamma=1.6$ meV.

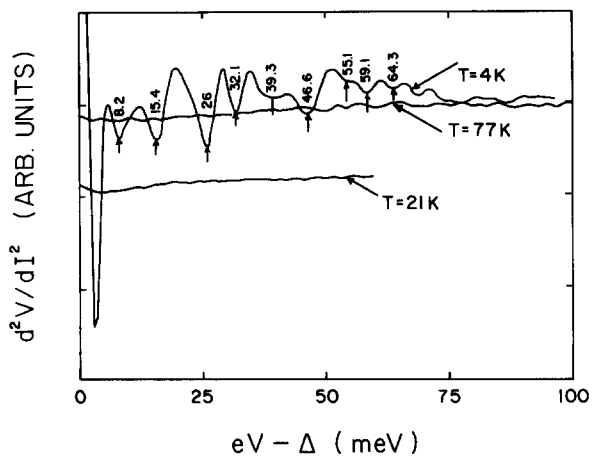

Fig. 8. d^2V/dI^2 vs. $eV-\Delta$ characteristic of the conductance curve shown in fig. 3. The gap (2.9 meV) was subtracted of the energy values. The numbers indicate the values of the dips in the curve at 4 K. Note that the structure disappears as the temperature increases from 4 to 77 K. The curve at 21 K was vertically moved for clarity.

malized to 18 K. Normalizing to 18 K is not arbitrary and is justified by the fact that at 18 K the tunneling characteristic dI/dV versus V shows normal state behavior. The solid line in this plot is the expected BCS behavior. Using the value of Δ obtained at 4 K (2.9 meV) and $T_c=18$ K, the ratio $2\Delta/K_BT_c$ is 3.75 indicating an intermediate-strong coupled BCS superconductor.

Figure 8 shows the d^2V/dI^2 versus energy $(eV-\Delta)$ characteristic of the conductance data shown in fig. 3. It is worth noting that this structure is symmetric with respect to voltage on both sides of the energy gap feature. The arrows indicate dips at approximately 8.2, 15.4, 26, 32.1, 39.3, 46.6, 55.1, 59.1, 64.3 meV, after subtracting the value for the energy gap (2.9 meV). This data can be correlated to the recently published inelastic neutron experiments reported by Loong et al. [14] and to the optical phonons that were observed by Raman spectroscopy [6].

It is interesting to mention that in the inelastic neutron experiments, two bands are observed at 30 and 60 meV, higher resolution neutron experiments may reveal fine structure in these bands, which are related to the softening of the oxygen phonon modes, according to molecular dynamics simulation (MD) MD calculations also show a band extending from 25 to 37 meV, peaks at 11, 15 and 51 meV, a shoulder at 16 meV, small peaks at 25, 46, 67 and 73 meV [14]. Practically all these features can be correlated one to one with our experimental tunneling results. Figure 8 also shows the d^2V/dI^2 curve taken at 21 and 77 K. We can observe that the structure totally disappears at 21 K, indicating that this is a characteristic of the superconducting state.

3. Conclusions

We can summarize the results of this research in the following points:

(1) We observed reproducible tunneling characteristics in junctions of $Ba_{0.6}K_{0.4}BiO_9$–insulator–Sn. The energy gap was found to be $\Delta = 2.9$ meV using a smeared density of states with $\Gamma = 1.6$ meV at 4 K.

(2) According to the ratio $2\Delta/k_BT_c$ the superconductor is in an intermediate coupled regime, which can be characterized in the framework of the BCS theory.

(3) The energy gap dependence with temperature follows the normal BCS behavior.

(4) The structure in the second derivative curve can be associated with phonon modes observed in recent neutron experiments.

Acknowledgements

This work was supported by the Programa Universitario de Superconductores Cerámicos de Alta Temperatura Crítica and by CONACYT. The work at Argonne was supported by the U.S. DOE, Basic Energy Sciences under Contrast No. W-31-109-ENG-38.

References

[1] L.F. Mattheis, E.M. Gyorgy and D.M. Johnson Jr., Phys. Rev. B37 (1988) 3745.
[2] R.J. Cava, B. Batlogg, J.J. Krajewski, R. Farrow, L.W. Rupp Jr., A.E. White, K. Short, W.F. Peck and T. Kometani, Nature 332 (1988) 814.
[3] D.G. Hinks, A.W. Mitchell, Y. Zheng, D.R. Richards and B. Dabrowsky, Appl. Phys. Lett. 54 (1989) 1585.
[4] D.G. Hinks, D.R. Richards, B. Dabrowski, D.T. Marx and A.W. Mitchell, Nature 335 (1988) 419.
[5] O. Navarro and R. Escudero, submitted for publication.
[6] K.F. McCarty, H.B. Radousky, D.G. Hinks, Y. Zheng, A.W. Mitchell, T.J. Folkerts and R.N. Shelton, Phys. Rev. B40 (1989) 2662.
[7] Z. Schlesinger, R.T. Collins, J.A. Calise, D.G. Hinks, A.W. Mitchell, Y. Zheng, B. Dabrowski, N.E. Bickers and D.J. Scalapino, Phys. Rev. B40 (1989) 6862.
[8] J.F. Zasadzinski, N. Tralshawala, D.G. Hinks, B. Dabrowski, A.W Mitchell and D.R. Richards, Physica C 158 (1989) 519.
[9] M. Gurvitch, J.M. Valles Jr., A.M. Cucolo, R.C. Dynes, J.P. Garno, L.F. Schneemeyer and J.V. Waszczak, Phys. Rev. Lett. 63 (1989) 1008.
[10] W.F. Brinkman, R.C. Dynes and J.M. Rowell, J. Appl. Phys. 41 (1970) 1915.
[11] J.F. Zasadzinski, N. Tralshawala, J. Timpf, D.G. Hinks, B. Dabrowski, A.W. Mitchell and D.R. Richards, Physica C 162–164 (1989) 1053.
[12] K. Nasu, Phys. Rev. B35 (1987) 1748;
K. Machida, T. Koyama and T. Matsubara, Phys. Rev. B23 (1981) 99.
[13] R.C. Dynes, V. Narayanamurti and J.P. Garno, Phys. Rev. Lett. 41 (1978) 1509.
[14] C.K. Loong, P. Vashishta, M.H. Degani, D.L. Price, J.D. Jorgensen, D.G. Hinks, B. Dabrowski, A.W. Mitchell, J.D. Richards and Y. Zheng, Phys. Rev. Lett. 62 (1989) 2628.